Human Molecular Genetics, 2013, Vol. 22, No. 16 **3218–3226**
doi:10.1093/hmg/ddt175
Advance Access published on April 10, 2013

The cataract and glucosuria associated monocarboxylate transporter MCT12 is a new creatine transporter

Jeannette Abplanalp[1,10], Endre Laczko[4], Nancy J. Philp[6], John Neidhardt[1], Jurian Zuercher[1], Philipp Braun[1], Daniel F. Schorderet[7,9], Francis L. Munier[8], François Verrey[2,3], Wolfgang Berger[1,3,5], Simone M.R. Camargo[2,3] and Barbara Kloeckener-Gruissem[1,10,*]

[1]Institute of Medical Molecular Genetics, [2]Institute of Physiology and [3]Zurich Center for Integrative Human Physiology, University of Zurich, Zurich, Switzerland, [4]Functional Genomics Center Zurich and [5]Neuroscience Center Zurich, University of Zurich/ETHZ, Zurich, Switzerland, [6]Department of Pathology, Anatomy and Cell Biology, Thomas Jefferson University, Philadelphia, PA, USA, [7]Institute for Research in Ophthalmology, Sion, Switzerland, University of Lausanne, Lausanne, Switzerland, [8]Jules-Gonin Eye Hospital, University of Lausanne, Lausanne, Switzerland, [9]Faculty of Life Sciences, École polytechnique fédérale de Lausanne, Lausanne, Switzerland and [10]Department of Biology, ETHZ, Zurich, Switzerland

Received February 18, 2013; Revised and Accepted April 8, 2013

Creatine transport has been assigned to creatine transporter 1 (CRT1), encoded by mental retardation associated *SLC6A8*. Here, we identified a second creatine transporter (CRT2) known as monocarboxylate transporter 12 (MCT12), encoded by the cataract and glucosuria associated gene *SLC16A12*. A non-synonymous alteration in MCT12 (p.G407S) found in a patient with age-related cataract (ARC) leads to a significant reduction of creatine transport. Furthermore, *Slc16a12* knockout (KO) rats have elevated creatine levels in urine. Transport activity and expression characteristics of the two creatine transporters are distinct. CRT2 (MCT12)-mediated uptake of creatine was not sensitive to sodium and chloride ions or creatine biosynthesis precursors, breakdown product creatinine or creatine phosphate. Increasing pH correlated with increased creatine uptake. Michaelis–Menten kinetics yielded a V_{max} of 838.8 pmol/h/oocyte and a K_m of 567.4 μM. Relative expression in various human tissues supports the distinct mutation-associated phenotypes of the two transporters. *SLC6A8* was predominantly found in brain, heart and muscle, while *SLC16A12* was more abundant in kidney and retina. In the lens, the two transcripts were found at comparable levels. We discuss the distinct, but possibly synergistic functions of the two creatine transporters. Our findings infer potential preventive power of creatine supplementation against the most prominent age-related vision impaired condition.

INTRODUCTION

Creatine is an essential component of the cellular energy household. It can either be synthesized by the body using the amino acids arginine, glycine and methionine or it can be supplied by nutrition. Creatine is transported to target cells via the bloodstream (1). After uptake into the cells, the phosphorylated form aids in immediate supply of ATP, especially under high demand of energy over a short period of time (2,3). Transport of creatine across the membrane requires the creatine transporter1, CRT1, which is encoded by *SLC6A8* located on the X chromosome (OMIN 300036). CRT1 consists of twelve transmembrane domains (4,5). Creatine uptake is saturable and requires sodium and chloride ions, enabling creatine transport against its concentration gradient (5,6). *SLC6A8* is most abundant in tissues with high energy demand including skeletal muscle, heart, brain and retina, but also in the intestine and kidney epithelial cells (7–9). In this context, it is interesting to

*To whom correspondence should be addressed at: Institute of Medical Molecular Genetics, University Zurich, Schorenstrasse 16, 8603 Schwerzenbach, Switzerland. Tel: +41 446557453; Fax: +41 446557213; Email: kloeckener@medgen.uzh.ch

note that mutations in *SLC6A8* primarily lead to mental retardation in male patients (OMIM 300352) (10–12), while kidney-related clinical features or those affecting vision have not been reported.

The fourteen members of the monocarboxylate transporter (MCT) family, encoded by the *SLC16* genes also contain 12 transmembrane domains (13). They display distinct expression patterns (14,15) and half of the MCT transporters, including MCT12 encoded by *SLC16A12* (OMIM 611910), are considered orphans (16). Substrates for the other half are diverse molecules including monocarboxylates, such as lactate, pyruvate and butyrate (MCT1, 2, 3 and 4) (17), thyroid hormones (MCT8) (18) or aromatic amino acids (MCT10/TAT1) (19,20). The localization of MCTs to the plasma membrane requires distinct accessory proteins, such as gp70/embigin for MCT2 or CD147/basigin for MCT1, 3, 4 and MCT12 (21–24). Based on the mutation analysis, the orphan transporter MCT12 is likely to play a role in energy metabolism, since a premature termination codon in the gene *SLC16A12* causes cataracts of the human lens and glucosuria with elevated, non-diabetic glucose levels in urine (OMIM 612018) (25,26). These findings suggest MCT12-mediated reduced reabsorption of glucose in the proximal convoluted tubules in kidney. Likewise, disturbed energy homeostasis within the avascular crystalline lens may result in opacities that cause cataracts. To be able to test this hypothesis, knowledge of the identity of the substrate is essential. To identify the substrate of MCT12, we combined the traditional heterologous *Xenopus laevis* oocyte expression system with a state-of-the-art metabolomics approach. Two possible candidates were experimentally tested and one of them, creatine, could be verified and characterized as a substrate for MCT12. This work demonstrates the existence of a second creatine transporter with distinct transport characteristics and expression patterns.

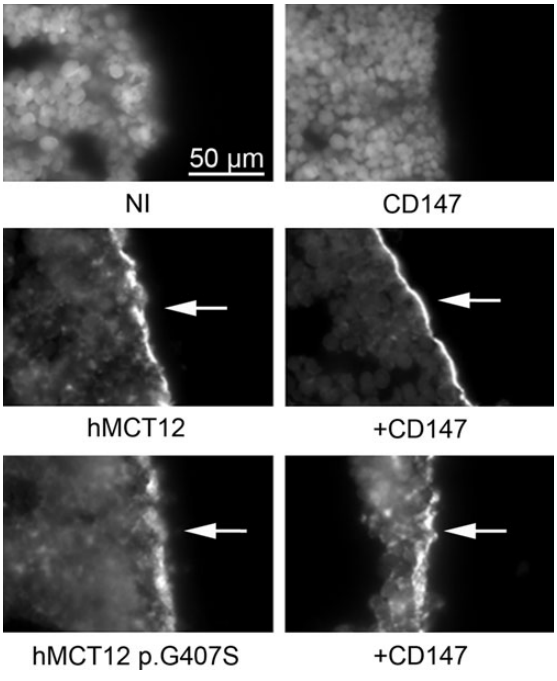

Figure 1. Immunofluorescence images. Membrane localization of human MCT12 (hMCT12) in *Xenopus laevis* oocytes injected with *SLC16A12* cRNA. Noninjected oocytes and those injected with the chaperone *CD147* alone served as controls (top row). Membrane localized signals (arrow) were detected only in oocytes injected with MCT12, irrespective of the presence of chaperone CD147.

RESULTS

Injection of *SLC16A12* cRNA leads to localization of MCT12 at the *Xenopus laevis* oocyte membrane

Xenopus laevis oocytes were chosen as the experimental system to investigate transport activity of MCT12. We either injected human reference or human mutant *SLC16A12* complementary RNA (cRNA). The presence or absence of coinjected chaperone *CD147* cRNA was also tested because the chaperone CD147 was shown to be necessary for proper localization of MCT12 in HEK293 cells. Injection of *CD147* cRNA alone served as a control. Under all conditions when the transporter was injected, a positive signal in the cell membrane was detected with MCT12-specific antibodies. These results were independent of the presence of the chaperone, suggesting that endogenous *Xenopus* CD147 homologue levels seem to be sufficient for MCT12 trafficking to the membrane. Oocytes injected with only the chaperone *CD147* cRNA did not yield a signal. As expected, noninjected oocytes also did not show a positive signal (Fig. 1). Specificity of the transporter signal was demonstrated by the use of the secondary antibody alone (Supplementary Material, Fig. S1A). The membrane marker isolectin B4 (IB4) was used to visualize the membranes in oocytes (Supplementary Material, Fig. S1B). Taken together, we concluded that the *Xenopus laevis* oocyte expression system provides the experimental requirements necessary to apply a metabolomics analysis in search for the MCT12 substrate.

Metabolomics approach suggested substrate candidates

A metabolomics approach was designed to narrow down the number of potential substrate candidates. Cell extracts obtained from oocytes that were either injected with *CD147* only (control) or coinjected with *CD147* and *SLC16A12* cRNA were subjected to the analysis of polar metabolites with liquid chromatography and mass spectrometry (LC-MS), which yielded 14′720 m/z values (ratio of ion mass (m) and its charge (z)). To exclude analytical and chemical noise, analysis was focused on m/z values corresponding to the known biological metabolites by application of a filter with the metabolites listed in the KEGG database (Kyoto Encyclopedia, www.genome.jp/kegg/, last accessed on 15 April 2013). This resulted in 553 metabolite hits. The observed intensity values of these metabolites were subjected to between-group-analysis (BGA), contrasting samples of injected oocyte lysates. This resulted in further reduction to 20 metabolites (Table 1). To evaluate these candidates, we considered the maximum fold change (log2 ratio) as well as statistical significance (two-way ANOVA). The two candidates, creatine (log2 ratio $= -2.6485$ and $P = 3.11 \times 10^{-7}$) and L-glutamine (log2 ratio $= 0.9945$ and $P = 0.0002$), displayed statistically highest significance. Furthermore, these candidates also belonged to the group of monocarboxylates and matched the physiological expectations of energy-related metabolites. Creatine yielded the most significant difference between oocytes injected with *CD147* cRNA alone and those coinjected with *CD147* and

Table 1. List of substrate candidates for MCT12 obtained from the metabolomic analysis

Metabolite	*P*-value two-way ANOVA with factors injection type and medium	Log2 ratio SLC16A12 injection over control (CD147)
ADP-ribose	0.1240	3.8570
L-glutamine	**0.0002**	**0.9945**
O-Acetyl-L-homoserine	0.0441	0.8344
7-Methyluric acid	0.0239	0.7736
Dihydromacarpine	0.3990	0.7188
3-Amino-2-oxopropyl phosphate	0.415	0.7082
N-((*R*)-Pantothenoyl)-L-cysteine	0.0424	0.7034
L-2,3-Dihydrodipicolinate	0.0100	0.6902
Cobalt-precorrin 7	0.0900	0.6101
CDP choline	0.1982	0.5996
(-Dihydroorotate	0.0990	−0.5854
1,4-Naphthoquinone	0.0990	−0.5854
CDP	0.0967	−0.6050
UDP glucuronate	0.3318	−0.6058
Salicin	0.0054	−0.6659
Benzo[a]pyrene-7,8-diol	0.0054	−0.6659
Cellopentaose	0.2726	−0.7048
5,6-Indolequinone-2-carboxylic acid	0.0002	−0.8816
3-Hydroxyanthranilate	8.93E−05	−0.9004
Creatine	**3.11E−07**	**−2.6485**

Statistical significance (two-way ANOVA) and fold change based on the observed intensity (log2 ratio).

SLC16A12 cRNA. The log2 ratio of −2.6485 corresponds to a 6.3-fold reduction in creatine levels ($P < 0.0001$, unpaired t-test) (Fig. 2A), suggesting efflux of creatine.

Efflux and uptake of creatine by MCT12

To test whether creatine was indeed specifically transported by MCT12, efflux experiments were performed, as suggested by the metabolomics study. The time course (0, 15 and 60 min) showed a significant increase in radioactivity (disintegrations per minute, DPM) ($P < 0.0001$, ANOVA) in the medium when oocytes were coinjected with the chaperone and *SLC16A12* cRNA (32 ± 3, 1805 ± 262, 6869 ± 636 DPM for the three time points, $n = 9$), verifying creatine efflux. Only minimal changes (ns, ANOVA) in the level of radioactivity were observed in noninjected (17 ± 1, 68 ± 34, 198 ± 100 DPM, $n = 9$) oocytes and those injected with the chaperone *CD147* cRNA alone (40 ± 17, 73 ± 21, 157 ± 57 DPM, $n = 10$). At time points 15 and 60, radioactivity in the medium of oocytes injected with the transporter was significantly different from the noninjected and chaperone only injected oocytes ($P < 0.0001$, ANOVA) (Fig. 2B). Remaining radioactivity in oocytes after the last time point was significantly reduced ($P < 0.0001$) in coinjected (12 165 ± 991 DPM) compared with noninjected (34 418 ± 951 DPM) and *CD147* only injected oocytes (31 958 ± 968 DPM, $n_{NI} = 10$, $n_{CD147} = 9$, $n_{CD147+hMCT12} = 8$) (Supplementary Material, Fig. S2). These results confirmed the data obtained from the metabolomics study and demonstrated that the efflux of creatine depends on MCT12. In an uptake experiment, we tested whether creatine transport is bidirectional. In oocytes expressing MCT12, creatine uptake was 195 ± 12 pmol/h/oocyte compared with 1 ± 0 pmol/h/oocyte and 1 ± 0 pmol/h/oocyte in the noninjected and CD147 only injected controls, respectively ($n = 10$ for each group) (Fig. 2C). The uptake of creatine was statistically significant compared with controls ($P < 0.0001$, ANOVA, followed by Tukey's test). Therefore, we conclude that MCT12 transports creatine into and out of a cell, probably depending on the creatine concentration gradient. Uptake experiments using L-glutamine as a substrate candidate did not yield MCT12 specificity (data not shown).

Characterization of creatine transport by MCT12

To investigate whether the uptake was dependent on the substrate concentration, different amounts of unlabeled creatine, ranging between 1 and 3000 μM, together with a constant concentration of ^{14}C creatine were used. The uptake profile followed typical Michaelis–Menten kinetics (Fig. 3A) with a V_{max} of 838.8 pmol/h/oocyte and a K_m of 567.4 μM. This uptake is specific to MCT12 as only the presence of MCT12 supported creatine uptake ($P \leq 0.0006$, for every concentration tested, unpaired *t*-test, $n = 7–10$ per concentration and experimental group) (Fig. 3A). Therefore, in the subsequent experiments, the values of CD147 only injected oocytes are considered background and will be subtracted from those obtained with MCT12. Creatine uptake by MCT12 was not dependent on Na^+ or Cl^- ions (ND96: 180 ± 13 pmol/h/oocyte, Na^+ free: 169 ± 8 pmol/h/oocyte and Cl^- free: 174 ± 16 pmol/h/oocyte, ($n = 19–25$ oocytes per group, $P = 0.8002$, ns, ANOVA) (Fig. 3B). Considering the pH (pH 7.4: 197 ± 13 pmol/h/oocte; pH 5.5: 154 ± 11 pmol/h/oocyte, pH 6.5: 178 ± 11 pmol/h/oocyte and pH 8.0 253 ± 15 pmol/h/oocyte; $n = 26–33$ per experimental group), creatine uptake was slightly reduced under more acidic conditions and significantly higher under more basic conditions ($P < 0.0001$, ANOVA, pH 8 versus pH 7.4, $P < 0.05$; pH 8 versus pH 6.5, $P < 0.001$ and pH 8 versus pH 5.5, $P < 0.001$, Tukey's test) (Fig. 3C). We further tested whether creatine precursors (arginine, glycine and ornithine), creatine breakdown product creatinine and the phosphorylated form of creatine interfere with creatine transport by MCT12. None of the tested compounds appeared to influence creatine uptake significantly ($P < 0.5358$, ANOVA) (Experiment 1: creatine only: 225 ± 25 pmol/h/oocyte, arginine: 165 ± 28 pmol/h/oocyte, glycine: 168 ± 27 pmol/h/oocyte, ornithine: 164 ± 34 pmol/h/oocyte and phosphocreatine: 169 ± 35 pmol/h/oocyte; ($n = 5–7$); Experiment 2: creatine only: 89 ± 9 pmol/h/oocyte), creatinine 95 ± 10 pmol/h/oocyte). To allow comparison of all compounds, the results are displayed as percentage in Figure 3D.

SLC16A12 mutation alters transport properties

In an *SLC16A12* mutation screen of patients with age-related cataracts (ARCs) we identified a novel heterozygous DNA sequence alteration (Fig. 4A) that maps to position c.1219G>A; p.G407S, affecting an evolutionary highly conserved amino acid that localizes to the last extracellular loop. This alteration was not found in 400 alleles from individuals representing the general population. Potential development of ARCs in this group is unlikely due to this sequence alteration. The patient with the c.1219G>A alteration was diagnosed

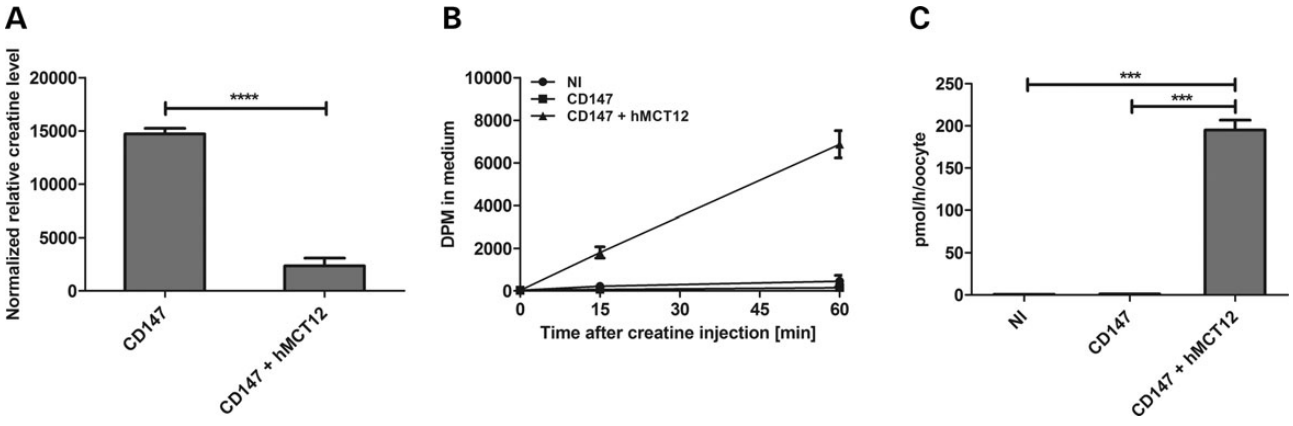

Figure 2. Creatine is transported by MCT12. (**A**) Significantly lower creatine levels (6.3-fold) were detected in oocytes coinjected with *SLC16A12* and its chaperone *CD147* compared with oocytes injected only with *CD147*. (**B**) Creatine efflux in noninjected oocytes (NI), and oocytes expressing CD147 or CD147 + hMCT12. Content of ^{14}C creatine in the medium was recorded as disintegrations per minute at different time points (0, 15 and 60 min). (**C**) Creatine uptake. Measurements were taken 10 min after addition of ^{14}C-creatine to the medium of oocytes (NI/CD147/CD147 + hMCT12). Uptake is shown as pmol/h/oocyte. Bars indicate SEM.

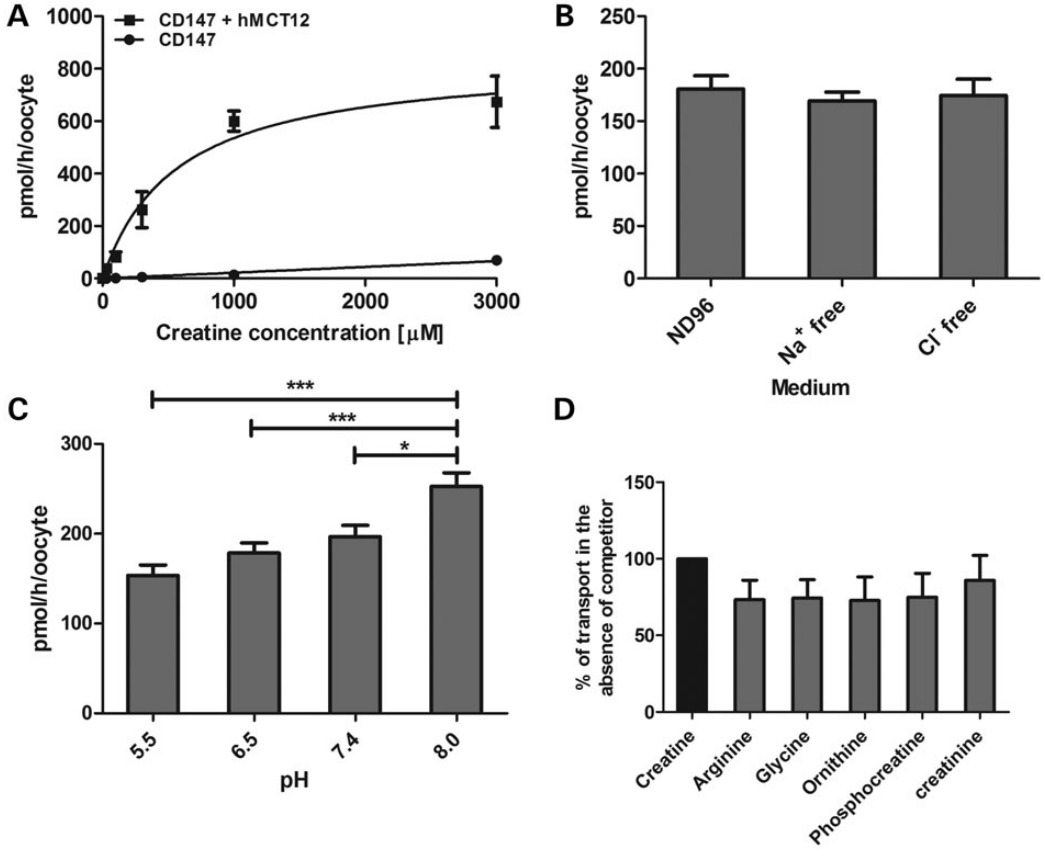

Figure 3. Characterization of creatine uptake. (**A**) Michaelis–Menten kinetics of creatine uptake. V_{max} = 838.8 pmol/h/oocyte and K_m = 567.4 μM. (**B**) Ion dependency of creatine uptake. Experiments were performed either in the presence of both sodium and chloride (NaCl) or in sodium (Na^+) or chloride (Cl^-)-free medium. (**C**) pH dependency of creatine uptake. pH of 5.5, 6.5, 7.4 and 8.0 were tested. (**D**) Effect of potential competitors on creatine uptake. Creatine uptake alone (creatine) is shown as 100%. Bars indicate SEM.

with bilateral nuclear cataract with radial cortical opacities in the left eye at the age of 69. To test whether this mutation interferes with creatine transport, we generated a construct of *SLC16A12* that carries this mutation and performed creatine uptake experiments as described above. Injection of mutated cRNA into *Xenopus laevis* oocytes leads to localization of MCT12 at the membrane (Fig. 1). Noticeably, the uptake of creatine was significantly lowered by 43% (reference MCT12: 146 ± 11 pmol/h/oocyte and mutant MCT12 p.G407S: 84 ± 9 pmol/h/oocyte, $P = 0.0004$, unpaired *t*-test) (Fig. 4B). The mechanism based on which the mutation alters creatine transport is not yet known.

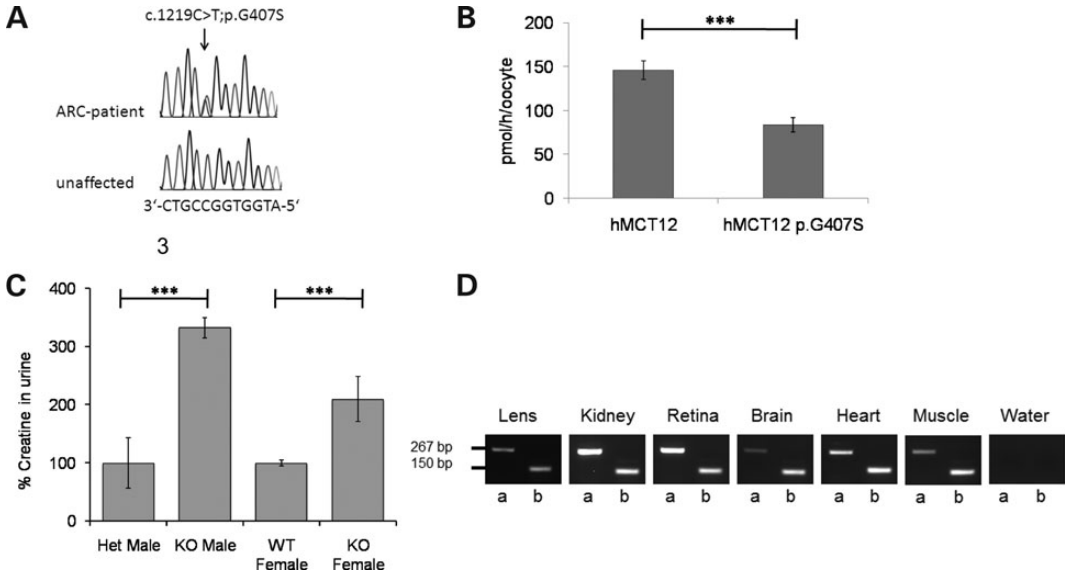

Figure 4. Effect of mutations on creatine transport and expression studies. (**A**) *SLC16A12* mutation screen. Electropherograms of an unaffected individual and of a patient with ARC showing the heterozygous mutation (arrow) *SLC16A12* c.1219G>A, p.G407S. (**B**) ^{14}C creatine uptake of oocytes expressing the mutant hMCT12 p.G407S compared with the reference hMCT12. The mutation causes a significant reduction in creatine uptake by 43% ($P = 0.0004$). Uptake was recorded as pmol/h/oocyte. Bars indicate SEM. (**C**) Creatine levels in urine of rats. Male *Slc16a12* KO or heterozygous (Het) rats and female KO and WT. Displayed are the percentages relative to the unaffected (not KO) males and females at 100%. Bars indicate SEM. (**D**) Expression of creatine transporter transcripts in human tissues. RT–PCR using primers specific for *SLC16A12* (a) and *SLC6A8* (b). Amplicon sizes are given in base pairs. Non-template control is water.

In rats, *Slc16a12* knockout (KO) animals did neither phenocopy the cataract nor the glucosuria phenotype (21), however creatine levels in the urine were significantly elevated (Fig. 4C). KO males accumulated 5.85 mM creatine compared with 1.76 mM in age-matched heterozygous KO males, which corresponds to an ∼3-fold difference. Likewise, an ∼2-fold difference was measured in females with 2.12 mM creatine in KO animals versus 1.01 mM in age-matched wild-type siblings. These results suggest that loss of *Slc16a12* results in the retention of creatine in the urine and a single copy of the gene is sufficient for creatine transport. Patients were not available for urine analysis.

Relative expression of *SLC16A12* and *SLC6A8* displayed tissue specificity

Expression of the two genes, *SLC16A12* and *SLC6A8*, encoding the creatine transporters, was investigated in various human tissues (Fig. 4D). Experimental conditions were chosen to allow assessment of the relative expression of the two transcripts within a given tissue, not necessarily between all tissues. In the lens, no striking difference was seen in the relative expression of both the transporters. However, in the kidney and retina, higher relative levels of *SLC16A12* were found. In brain, heart and muscle tissue, *SLC6A8* was more abundant. We concluded that tissue-specific differences in gene expression exist, which are likely to reflect the respective physiological functions.

DISCUSSION

The use of a metabolomics approach in combination with the heterologous *Xenopus laevis* oocyte expression system resulted in the identification of creatine as the substrate for the solute carrier MCT12. This novel combination of technologies is a powerful tool and our results open opportunities for substrate identification of many of the remaining orphan transporters. Furthermore, application of creatine may provide potential means of prevention of ARCs.

Characteristics of the transporters

Until now, the only creatine transporter characterized is CRT1. Here, we present the findings of a second creatine transporter CRT2, known as MCT12. While the structural similarities of both the transporters include the presence of 12 transmembrane domains (25,27), their activity profile is quite distinct. In contrast to MCT12, which performs facilitated transport of creatine, likely along a concentration gradient, CRT1 requires sodium and chloride ions and works against the creatine concentration gradient (4,5,10). CRT1 is encoded by *SLC6A8* on the X chromosome (4,10) and mutations in *SLC6A8* lead to mental retardation often combined with speech delay and epileptic conditions, but also with muscular dystrophy (10–12). The expression patterns of the two creatine transporters are also distinct: the predominant expression of CRT1 transcripts in the brain may correlate well with the observed clinical symptoms of severe developmental delays in patients with deficiencies in *SLC6A8* (28,29). Among the various deficiencies in patients with *SLC6A8* mutations, cataracts, microcornea or glucosuria were not reported. The latter symptoms are seen in patients with mutations in *SLC16A12* (25) but, in turn, these patients did not show obvious signs of developmental delay or other neurological disorders. Possibly, predominant expression of *SLC16A12* compared with *SLC6A8* in kidney may help to explain this observation. Initial data on membrane localization of the two creatine transporters indicate that they occupy opposing sides of epithelial cells; MCT12 seems predominantly at the basolateral membrane in lens (21), while

CRT1 was found at the apical membrane in proximal tubule cell lines and the proximal tubule in rats (8). A possible explanation for transepithelial transport of creatine could be envisioned in analogy to the paired transport system described for broad specificity, Na^+-independent neutral and cation ionic amino acid transporter (30). The absence of MCT12 but the presence of CRT1 in the proximal convoluted tubule of the kidney of the *Slc16a12* KO rat would help explain the observed increase spillage of creatine into the urine. It is not uncommon that mutations in genes that are more generally expressed cause highly specific clinical symptoms. Whether differences in function or expression or both are responsible for the activity of the two transporters need to await further experiments.

Proper maturation and localization of MCTs require chaperones (22–24) and in HEK293 cells CD147 assumes this task for MCT12 (21). In *Xenopus laevis* oocytes, the endogenous level of the CD147 homolog (22) seems sufficient to properly guide the transporter to the membrane. The proton environment is known to affect transport activity and pH sensitivity known of other members of the MCT family (31) also applies to MCT12, such that creatine transport is significantly increased under basic conditions. As MCT12 localizes to the lens cortex (21), these findings correlate well with a pH gradient in the lens of a more acidic core and a more basic cortex (32–34).

Aside from MCT12's involvement in cataract, microcornea and glucosuria, little is known on its function and biology. Recently it was reported as a biomarker for prostate, colon and breast cancers (35). A role of creatine in cancerous tissues is not surprising, given that tumor growth is a high energy-consuming process.

Function of the substrate creatine

Creatine is best known for its capacity as energy buffer via phosphocreatine (PCr) (2). High levels of PCr are found in skeletal muscle, brain and retina (3) and its presence in the lens was established by NMR studies (36), which implies a possible contribution to the energy demand in this avascular structure. As differentiated lens fiber cells mainly use glycolysis as an energy source and do not have any direct oxygen supply from blood vessels (37), an energy buffer such as creatine could be advantageous. In this context, the cataract phenotype in patients with mutations in *SLC16A12* might be explained via altered properties of creatine transport leading to disturbance of energy metabolism and resulting in structural changes and opacities within the lens. The relatively high level of PCr in human lens compared with other mammals (36) may indicate species-specific variation in its function, which may have contributed to the lack of cataracts in *Slc16a12* KO rats (21).

Furthermore, creatine was found to have antioxidative function (38), which could be beneficial to the aging cell. It could act as a mild antioxidant in the lens, which is exposed to environmental and molecular factors of oxidative stress (i.e. glutathione) (39). The fact that age-related processes like ARC are affected by MCT12 (40) supports this point. In addition, creatine also functions as cytoprotective, anti-apoptotic reagent (41,42). In the lens, an attenuated apoptotic-like process leads to loss of organelles as part of the differentiating process (43) and creatine might play a role in this attenuated process.

Within the kidney, the involvement of creatine in glucosuria could be envisioned with focus on the action of the Na^+-K^+-ATPase. It generates a sodium gradient, which is required for glucose reabsorption in the kidney proximal tubule performed by secondary activity of the sodium-glucose linked transporters SGLT1 and 2 (44). As PCr is able to support maximal pump function of the Na^+-K^+-ATPase in kidney cells (45), a possible hypothesis is that disturbance of creatine transport could lead to inefficient glucose reabsorption. Alternatively, at a cellular level, renal glucosuria could be a response to ER stress, followed by the unfolded protein response, as this pathway was recently suggested to influence central metabolic processes, particularly glucose metabolism (46). In support is our previously reported finding that the *SLC16A12* premature termination mutation in patients with renal glucosuria (25) elicits UPR in cell culture (21).

Taken together, the here reported findings will further our understanding of creatine homeostasis and the role of both transporters during this process. Upon further investigations, creatine may become a preventive supplement for the most prevalent age-related vision impairment, cataracts.

MATERIALS AND METHODS

Cloning

The following constructs were generated for the purpose of expression in the heterologous *Xenopus laevis* oocyte system. All restriction enzymes were purchased from Fermentas (St. Leon-Rot, DE), unless otherwise stated. As vector we used the BlueScript derived vector KSM (provided by Leila Virkki). The correct DNA sequence of all cloned inserts was verified by Sanger sequencing. For human reference *SLC16A12* (ENST00000341233; protein Q6ZSM3) a partial sequence in EST clone IRAKp961C20200Q (imaGenes) was completed using complementary DNA (cDNA) gained from HEK293 cells. Isolated RNA (RNeasy Kit; Qiagen) was treated with DNase and reverse transcribed using random hexamers for priming and SuperScript III (Invitrogen). An RT–PCR with a template mixture of clone IRAKp961C20200Q and cDNA, primers SLC16A12_CL1_for and CL2.2_rev (Supplementary Material, Table S1) and Pfu DNA polymerase (Promega) were incubated (95°C 2 min; 94°C 1 min; 55°C 30 s; 72°C 4 min; ×40; 72°C 5 min). Human mutation SLC16A12 (c.1219G>A) was generated by site-directed mutagenesis with the reference clone as a template and primers SLC16A12_CL1_for, MCT12_1219A_long_f, MCT12_1219T_long_r and SLC16A12_CL2.2_rev, specific for the sequence alteration (Supplementary Material, Table S1) and cloned into KSM. The mouse CD147-pOTB7 cDNA was acquired from IMAGE consortium (3589236) and subcloned with *Sal*I/*Not*I into the pCMV-sport6 expression vector.

In vitro transcription

KSM clones were linearized with *Sac*II. CD147-pCMV-sport6 was linearized with *NheI*. *In vitro* transcription was performed using the respective MEGAscript® kit (Ambion).

Xenopus laevis ooctes and injections

Oocytes were surgically removed from *Xenopus laevis* and treated as described (20). For injection, a Nanoject II microinjector (Drummond) was used. A minimum of five oocytes were injected for each experimental condition. Injection volume was 50 nl. The amount of cRNA was 10 ng for CD147 and 20 ng for the transporter. Oocytes were kept at 18°C in ND96 medium supplemented with 5 mg/l doxycycline and gentamycin, each. For efflux, 100 mM creatine supplemented with 10 nCi of ^{14}C radiolabeled creatine (Hartmann Analytic) was injected 3 days after cRNA injection. Oocytes were incubated at 25°C in ND96 (please refer Supplementary Material, Table S1, for medium compositions). Medium aliquots were removed and radioactivity was measured using Emulsifier-Safe™ scintillation cocktail (PerkinElmer) and a Tri-Carb 2900TR Liquid Scintillation Analyzer (Packard). Efflux was stopped by washing the oocytes with ND96. Oocytes were lysed with sodium dodecyl sulphate (SDS) and radioactivity was measured. For uptake, 3 days after injection, oocytes were washed with ND96 and incubated at 25°C for 2 min. ND96 was replaced with 100 μM uptake solution (concentrations ranging from 1 to 3000 μM were used for Michaelis–Menten kinetics), supplemented with 0.2 μCi ^{14}C-radiolabeled creatine. After 10 min, uptake was stopped by removing the uptake solution followed by washing the oocytes with ND96. The oocytes were further processed as described for the efflux experiments and radioactivity measured. For competition uptake experiments, in addition to creatine, 1 mM of arginine, glycine, ornithine, phosophocreatine and creatinine was added. For ion- and pH dependency experiments, modified ND96 media supplemented with creatine were used (Supplementary Material, Table S2). Results from all efflux and uptake experiments were statistically analyzed and plotted using Prism software (http://www.graphpad.com/scientific-software/prism/, last date accessed on 15 April 2013). Unpaired tests or Michaelis–Menten kinetics were applied. Confidence intervals were calculated and included in the graphs.

Cryosectioning

Three days after injection of cRNA, oocytes were washed in phosphate buffered saline (PBS) (Gibco) and fixed for 2 h in 4% paraformaldehyde at 4°C and incubated at 4°C in 30% sucrose overnight. Three to five oocytes were placed in a 10 × 10 × 5 mm Tissue-Tek® Cryomold® (Sakura Finetek) filled with Tissue-Tek® (Sekura Finetek) and 7 μm sections were cut using a CM3050 S cryostat (Leica). Sections were placed on SuperFrost® slides and stored overnight at −20°C.

Immunofluorescence

Cryosections were blocked for 1 h [PBS containing 0.05% Tween (PBST) and 1% BSA (Sigma)]. Antibodies against the C-terminal end of human MCT12 (21) (dilution 1:500) and the *Bandeiraea simplicifolia* isolectin B4 FITC conjugate (IB4-FITC, Sigma) (dilution 1:100) were applied and the slides incubated overnight at 4°C. Samples treated with IB4-FITC were mounted using Fluoromount (Sigma) and coverslips (44). Samples treated with the MCT12 antibody were incubated with secondary goat anti-rabbit IgG Alexa Fluor® 488 (Invitrogen) (1:200 dilution) (60 min) and mounted. Samples treated with the secondary antibody only were included as control. Pictures were recorded on an Axioplan 2 imaging system (Zeiss) with an Axiocam MRm camera (Zeiss) and processed with Photoshop CS4 (Adobe).

Transcript analysis

RNA of human tissues was obtained from Takara Bio Europe/Clontech (Saint-Germain-en-Laye, France). Reverse transcription was performed using Superscript III (Invitrogen). RT–PCR was carried out using an annealing temperature of 60°C and 32 cycles for *SLC6A8* (primer pair SLC6A8 hum ex6up and SLC6A8 hum ex5dn amplifying a fragment of 150 bp) and *SLC16A12* (primer pair SLC16A12 RNA 4/5f and SLC16A8 RNA 6r). Lens RNA from a donor eye was 3 fold concentrated using the concentrator 5301 from Eppendorf prior to reverse transcription treatment. Resulting cDNA required 41 cycles in RT–PCR (25).

Creatine assay

Urine was collected from wild-type (3 female), *Slc16a12*$^{+/-}$ (3 male) and *Slc16a12*$^{-/-}$ (3 female and 3 male) rats, then centrifuged at 3000*g* for 10 min to remove any particulate matter. Supernatants were taken and stored at −80°C. The levels of creatine in the urine of wild-type, heterozygous and homozygous *Slc16a12* male and female rats were measured using the creatine assay kit from BioVision.

Metabolomics

Sample preparation and handling

Oocytes were coinjected with SLC16A12 plus CD147 or with CD147 alone and incubated for 2 days. At this point, 20 oocytes per condition were incubated for additional 2 days in either ND96 or rich medium (Supplementary Material, Table S3), which was supplemented with metabolites mimicking human plasma (47,48) and Kao and Michayluk vitamin mix (Sigma) (49). Oocytes were lysed in ND96 supplemented with protease inhibitors (Sigma). Samples were centrifuged (4°C; 25 000 rcf; 5 min). The supernatant was subjected to repeated (2×) centrifugation and concentrated to a final volume of 100 μl. For LC-MS analysis, three aliquots of 20 μl of the oocyte lysates were diluted (1:5) with 50 mM ammonium acetate in acetonitrile/methanol/water/saturated aqueous ammonium hydroxide (900:90:9:1,v/v, pH 9). All reagents, reference compounds and internal standards were purchased from Sigma-Aldrich Fluka (Buchs, Switzerland). LiChrosolv grade organic solvents for LC and sample dilution were obtained from Merck (Darmstadt, Germany) and HPLC grade water was obtained from Sigma-Aldrich (Steinheim, Germany). Hydrophilic interaction chromatography was performed on a nano-UPLC system (Waters Inc. Milford, USA). Mobile phase A was 0.5 mM ammonium acetate in water/saturated aqueous ammonium hydroxide (998:2,v/v, pH 9) and mobile phase B was 0.5 mM ammonium acetate in acetonitrile/water/saturated aqueous ammonium hydroxide (950:48:2,v/v, pH 9). A solvent gradient starting from 10%A at initial run time to 50%A at

10 min run time was applied. The initial flow rate of 6 μl/min was lowered to 4 μl/min at 10 min run time. The run was completed by a washing phase of 4 min at 10%A. Selfmade spray tip columns of 150 × 0.2 mm, packed with Waters BEH Amide type solid phase (1.7 μm average particle size), were used.

The UPLC system was coupled by a nano-ESI source to a Synapt G2 HDMS (Waters, Manchester, UK). Negative mode MS^E data over a mass range of 50–1200 m/z were acquired with a rate of 3 spectra/sec for the entire UPLC run. Leucine enkephalin (2 ng/μL in acetonitrile/water 50:50 v/v with 0.1% formic acid v/v) was used as internal lock mass.

Data processing and data analysis

Centroided MS data (function 1 of the acquired MS^E data) were processed by MarkerLynx XS 4.1 (Waters, Manchester, UK) to obtain a primary list of $[M\text{-}H]^-$ ions detected in any of the samples, together with its intensity in all samples. This primary list was searched in a database with a mass tolerance of 50 mDa and with the assumption that all metabolites only form $[M-H]^-$ ions. A custom MarkerLynx database containing 3166 exact mass values, metabolite IDs, molecular formulas and pathway information of all KEGG listed metabolites (http://www.genome.jp/kegg/) was queried. The resulting annotated spectral intensity data matrix of the form *n* detected masses × *p* samples was imported in an R workspace (www.r-project.org, last accessed on 15 April 2013) to perform descriptive statistics, univariate and multivariate data analyses. BGA based on correspondence analysis (CoA) was used to detect and visualize metabolites affected by the experimental conditions, i.e. potentially transported across the oocyte membrane (R library made4, (50)). The intensity data for the top candidates detected by BGA were additionally analyzed by one-way as well as two-way ANOVA (as appropriate) and visualized by boxplots.

SLC16A12 mutation screen

Patients with ARCs were seen by an ophthalmologist (FM) and they gave informed consent. The study conformed to the standards set by the Declaration of Helsinki, Conditions for the DNA mutation screen have been described (40). Control individuals represent the general population; they were not age-matched and may develop ARC.

SUPPLEMENTARY MATERIAL

Supplementary Material is available at *HMG* online.

ACKNOWLEDGEMENTS

We thank David Fischer (FGCZ) for performing the LC-MS analysis and data pre-processing, Lukas Bock and Eva Hänsenberger (Institute of Physiology) for assistance with *Xenopus laevis* oocyte experiments; Romain Da Costa, Istvan Magyar and Esther Glaus (Institute of Medical Molecular Genetics) for help with image and graphic technology and immunohistochemistry.

Conflict of Interest statement. None declared.

FUNDING

Support from National Institutes of Health (grant EY-012042 to N.J.P.) is appreciated; transcript analysis was supported by Velux foundation to J.N.

REFERENCES

1. Walker, J.B. (1979) Creatine: biosynthesis, regulation, and function. *Adv. Enzymol. Relat. Areas Mol. Biol.*, **50**, 177–242.
2. Wallimann, T., Wyss, M., Brdiczka, D., Nicolay, K. and Eppenberger, H.M. (1992) Intracellular compartmentation, structure and function of creatine kinase isoenzymes in tissues with high and fluctuating energy demands: the phosphocreatine circuit' for cellular energy homeostasis. *Biochem. J.*, **281**(Pt 1), 21–40.
3. Wallimann, T., Tokarska-Schlattner, M. and Schlattner, U. (2011) The creatine kinase system and pleiotropic effects of creatine. *Amino Acids*, **40**, 1271–1296.
4. Fitch, C.D., Shields, R.P., Payne, W.F. and Dacus, J.M. (1968) Creatine metabolism in skeletal muscle. 3. Specificity of the creatine entry process. *J. Biol. Chem.*, **243**, 2024–2027.
5. Dai, W., Vinnakota, S., Qian, X., Kunze, D.L. and Sarkar, H.K. (1999) Molecular characterization of the human CRT-1 creatine transporter expressed in Xenopus oocytes. *Arch. Biochem. Biophys.*, **361**, 75–84.
6. Loike, J.D., Somes, M. and Silverstein, S.C. (1986) Creatine uptake, metabolism, and efflux in human monocytes and macrophages. *Am. J. Physiol.*, **251**, C128–C135.
7. Guimbal, C. and Kilimann, M.W. (1993) A Na(+)-dependent creatine transporter in rabbit brain, muscle, heart, and kidney. cDNA cloning and functional expression. *J. Biol. Chem.*, **268**, 8418–8421.
8. Li, H., Thali, R.F., Smolak, C., Gong, F., Alzamora, R., Wallimann, T., Scholz, R., Pastor-Soler, N.M., Neumann, D. and Hallows, K.R. (2010) Regulation of the creatine transporter by AMP-activated protein kinase in kidney epithelial cells. *Am. J. Physiol. Renal Physiol.*, **299**, F167–F177.
9. Peral, M.J., García-Delgado, M., Calonge, M.L., Durán, J.M., De La Horra, M.C., Wallimann, T., Speer, O. and Ilundáin, A.A. (2002) Human, rat and chicken small intestinal Na+-Cl−-creatine transporter: functional, molecular characterization and localization. *J. Physiol.*, **545**, 133–144.
10. Gregor, P., Nash, S.R., Caron, M.G., Seldin, M.F. and Warren, S.T. (1995) Assignment of the creatine transporter gene (SLC6A8) to human chromosome Xq28 telomeric to G6PD. *Genomics*, **25**, 332–333.
11. Salomons, G.S., van Dooren, S.J., Verhoeven, N.M., Marsden, D., Schwartz, C., Cecil, K.M., DeGrauw, T.J. and Jakobs, C. (2003) X-linked creatine transporter defect: an overview. *J. Inherit. Metab. Dis.*, **26**, 309–318.
12. Betsalel, O.T., Pop, A., Rosenberg, E.H., Fernandez-Ojeda, M., Jakobs, C. and Salomons, G.S. (2012) Detection of variants in SLC6A8 and functional analysis of unclassified missense variants. *Mol. Genet. Metab.*, **105**, 596–601.
13. Meredith, D. and Christian, H.C. (2008) The SLC16 monocaboxylate transporter family. *Xenobiotica*, **38**, 1072–1106.
14. Halestrap, A.P. and Price, N.T. (1999) The proton-linked monocarboxylate transporter (MCT) family: structure, function and regulation. *Biochem. J.*, **343**(Pt 2), 281–299.
15. Halestrap, A.P. and Wilson, M.C. (2012) The monocarboxylate transporter family—role and regulation. *IUBMB Life*, **64**, 109–119.
16. Fredriksson, R., Nordstrom, K.J., Stephansson, O., Hagglund, M.G. and Schioth, H.B. (2008) The solute carrier (SLC) complement of the human genome: phylogenetic classification reveals four major families. *FEBS Lett.*, **582**, 3811–3816.
17. Halestrap, A.P. (2012) The monocarboxylate transporter family—structure and functional characterization. *IUBMB Life*, **64**, 1–9.
18. Friesema, E.C., Ganguly, S., Abdalla, A., Manning Fox, J.E., Halestrap, A.P. and Visser, T.J. (2003) Identification of monocarboxylate transporter 8 as a specific thyroid hormone transporter. *J. Biol. Chem.*, **278**, 40128–40135.
19. Kim, D.K., Kanai, Y., Chairoungdua, A., Matsuo, H., Cha, S.H. and Endou, H. (2001) Expression cloning of a Na+-independent aromatic amino acid transporter with structural similarity to H+/monocarboxylate transporters. *J. Biol. Chem.*, **276**, 17221–17228.
20. Ramadan, T., Camargo, S.M., Summa, V., Hunziker, P., Chesnov, S., Pos, K.M. and Verrey, F. (2006) Basolateral aromatic amino acid transporter

TAT1 (Slc16a10) functions as an efflux pathway. *J. Cell Physiol.*, **206**, 771–779.
21. Castorino, J.J., Gallagher-Colombo, S.M., Levin, A.V., Fitzgerald, P.G., Polishook, J., Kloeckener-Gruissem, B., Ostertag, E. and Philp, N.J. (2011) Juvenile cataract-associated mutation of solute carrier SLC16A12 impairs trafficking of the protein to the plasma membrane. *Invest. Ophthalmol. Vis. Sci.*, **52**, 6774–6784.
22. Kirk, P., Wilson, M.C., Heddle, C., Brown, M.H., Barclay, A.N. and Halestrap, A.P. (2000) CD147 is tightly associated with lactate transporters MCT1 and MCT4 and facilitates their cell surface expression. *EMBO J.*, **19**, 3896–3904.
23. Philp, N.J., Ochrietor, J.D., Rudoy, C., Muramatsu, T. and Linser, P.J. (2003) Loss of MCT1, MCT3, and MCT4 expression in the retinal pigment epithelium and neural retina of the 5A11/basigin-null mouse. *Invest. Ophthalmol. Vis. Sci.*, **44**, 1305–1311.
24. Wilson, M.C., Meredith, D., Fox, J.E., Manoharan, C., Davies, A.J. and Halestrap, A.P. (2005) Basigin (CD147) is the target for organomercurial inhibition of monocarboxylate transporter isoforms 1 and 4: the ancillary protein for the insensitive MCT2 is EMBIGIN (gp70). *J. Biol. Chem.*, **280**, 27213–27221.
25. Kloeckener-Gruissem, B., Vandekerckhove, K., Nurnberg, G., Neidhardt, J., Zeitz, C., Nurnberg, P., Schipper, I. and Berger, W. (2008) Mutation of solute carrier SLC16A12 associates with a syndrome combining juvenile cataract with microcornea and renal glucosuria. *Am. J. Hum. Genet.*, **82**, 772–779.
26. Vandekerckhove, K., Lange, A.P., Herzog, D. and Schipper, I. (2007) Juvenile cataract associated with microcornea and glucosuria: a new syndrome. *Klin Monbl Augenheilkd*, **224**, 344–346.
27. Yamashita, A., Singh, S.K., Kawate, T., Jin, Y. and Gouaux, E. (2005) Crystal structure of a bacterial homologue of Na+/Cl-dependent neurotransmitter transporters. *Nature*, **437**, 215–223.
28. Nasrallah, F., Feki, M. and Kaabachi, N. (2010) Creatine and creatine deficiency syndromes: biochemical and clinical aspects. *Pediatr. Neurol.*, **42**, 163–171.
29. Salomons, G.S., van Dooren, S.J., Verhoeven, N.M., Cecil, K.M., Ball, W.S., Degrauw, T.J. and Jakobs, C. (2001) X-linked creatine-transporter gene (SLC6A8) defect: a new creatine-deficiency syndrome. *Am. J. Hum. Genet.*, **68**, 1497–1500.
30. Bauch, C., Forster, N., Loffing-Cueni, D., Summa, V. and Verrey, F. (2003) Functional cooperation of epithelial heteromeric amino acid transporters expressed in madin-darby canine kidney cells. *J. Biol. Chem.*, **278**, 1316–1322.
31. Broer, S., Schneider, H.P., Broer, A., Rahman, B., Hamprecht, B. and Deitmer, J.W. (1998) Characterization of the monocarboxylate transporter 1 expressed in Xenopus laevis oocytes by changes in cytosolic pH. *Biochem. J.*, **333**(Pt 1), 167–174.
32. Bassnett, S. and Duncan, G. (1988) The influence of pH on membrane conductance and intercellular resistance in the rat lens. *J. Physiol.*, **398**, 507–521.
33. Mathias, R.T., Riquelme, G. and Rae, J.L. (1991) Cell to cell communication and pH in the frog lens. *J. Gen. Physiol.*, **98**, 1085–1103.
34. Stewart, S., Duncan, G., Marcantonio, J.M. and Prescott, A.R. (1988) Membrane and communication properties of tissue cultured human lens epithelial cells. *Invest. Ophthalmol. Vis. Sci.*, **29**, 1713–1725.
35. Chung, W., Kwabi-Addo, B., Ittmann, M., Jelinek, J., Shen, L., Yu, Y. and Issa, J.P. (2008) Identification of novel tumor markers in prostate, colon and breast cancer by unbiased methylation profiling. *PLoS ONE*, **3**, e2079.
36. Kopp, S., Glonek, T. and Greiner, J. (1982) Interspecies variations in mammalian lens metabolites as detected by phosphorus-31 nuclear magnetic resonance. *Science*, **215**, 1622–1625.
37. Dahm, R., van Marle, J., Quinlan, R.A., Prescott, A.R. and Vrensen, G.F. (2011) Homeostasis in the vertebrate lens: mechanisms of solute exchange. *Philos. Trans. R. Soc. Lond. B Biol. Sci.*, **366**, 1265–1277.
38. Sestili, P., Martinelli, C., Colombo, E., Barbieri, E., Potenza, L., Sartini, S. and Fimognari, C. (2011) Creatine as an antioxidant. *Amino Acids*, **40**, 1385–1396.
39. Mathias, R.T., Kistler, J. and Donaldson, P. (2007) The lens circulation. *J. Membr. Biol.*, **216**, 1–16.
40. Zuercher, J., Neidhardt, J., Magyar, I., Labs, S., Moore, A.T., Tanner, F.C., Waseem, N., Schorderet, D.F., Munier, F.L., Bhattacharya, S. *et al.* (2010) Alterations of the 5′untranslated region of SLC16A12 lead to age-related cataract. *Invest. Ophthalmol. Vis. Sci.*, **51**, 3354–3361.
41. O'Gorman, E., Beutner, G., Dolder, M., Koretsky, A.P., Brdiczka, D. and Wallimann, T. (1997) The role of creatine kinase in inhibition of mitochondrial permeability transition. *FEBS Lett.*, **414**, 253–257.
42. Dolder, M., Walzel, B., Speer, O., Schlattner, U. and Wallimann, T. (2003) Inhibition of the mitochondrial permeability transition by creatine kinase substrates. Requirement for microcompartmentation. *J. Biol. Chem.*, **278**, 17760–17766.
43. Bassnett, S. (2009) On the mechanism of organelle degradation in the vertebrate lens. *Exp. Eye Res.*, **88**, 133–139.
44. Vallon, V., Platt, K.A., Cunard, R., Schroth, J., Whaley, J., Thomson, S.C., Koepsell, H. and Rieg, T. (2011) SGLT2 mediates glucose reabsorption in the early proximal tubule. *J. Am. Soc. Nephrol.*, **22**, 104–112.
45. Guerrero, M.L., Beron, J., Spindler, B., Groscurth, P., Wallimann, T. and Verrey, F. (1997) Metabolic support of Na+ pump in apically permeabilized A6 kidney cell epithelia: role of creatine kinase. *Am. J. Physiol.*, **272**, C697–C706.
46. Wang, X., Eno, C.O., Altman, B.J., Zhu, Y., Zhao, G., Olberding, K.E., Rathmell, J.C. and Li, C. (2011) ER stress modulates cellular metabolism. *Biochem. J.*, **435**, 285–296.
47. Samuelsson, M., Vainikka, L. and Öllinger, K. (2011) Glutathione in the blood and cerebrospinal fluid: a study in healthy male volunteers. *Neuropeptides*, **45**, 287–292.
48. Shih, VE. (1996) In Blau, N.A.B. and Blaskovics, M.E. (eds), *Physician's Guide to the Laboratory Diagnosis of Metabolic Disease*, Chapman & Hall, London, pp. 13–30.
49. Davey, M.R., Anthony, P., Power, J.B. and Lowe, K.C. (2006) Isolation, culture, and plant regeneration from leaf protoplasts of Passiflora. *Methods Mol. Biol.*, **318**, 201–210.
50. Culhane, A.C., Perriere, G., Considine, E.C., Cotter, T.G. and Higgins, D.G. (2002) Between-group analysis of microarray data. *Bioinformatics*, **18**, 1600–1608.